6th International Symposium on High-Temperature Metallurgical Processing
Edited by: Tao Jiang, Jiann-Yang Hwang, Gerardo R. F. Alvear F., Onuralp Yücel, Xinping Mao, Hong Yong Sohn, Naiyang Ma, Phillip J. Mackey, and Thomas P. Battle
TMS (The Minerals, Metals & Materials Society), 2015

SEPARATION OF NON-METALLIC INCLUSIONS FROM ALUMINUM MELT BY SUPER GRAVITY

Gaoyang Song[1,2], Bo Song[1,2], Yuhou Yang[1,2], Shujian Jia[1,2], Mingming Song[1,2]

[1]School of Metallurgical and Ecological Engineering, University of Science and Technology Beijing, Xueyuan Road 30, Haidian District, Beijing 100083, China;
[2]State Key Laboratory of Advanced Metallurgy, University of Science and Technology Beijing, Xueyuan Road 30, Haidian District, Beijing 100083, China;

Keywords: Al melt, Non-metallic inclusions, Super gravity, Separation

Abstract

An innovative method is investigated to separate inclusion particles from liquid metal by super gravity. To make clear the characteristics of the inclusion separation, Al melt containing $MgAl_2O_4$ particles with diameters less than 150 μm has been treated under various super-gravity fields. The thickness of particle-accumulated layer formed at the bottom of the sample and the area fraction, number density and size of inclusions were measured. It is found that the thickness of the particle-accumulated layer decreases and the area fraction of particles at this location increases with the increase of super-gravity field. With the gravity coefficient G=500, time t=2 min, and temperature T=1023 K, it is hardly to find any solid particles in the upper and middle areas of the sample and the separation efficiency is up to 90%.

Introduction

It is well known that non-metallic inclusions in the aluminum alloy can not only increase melt viscosity, but also reduce the casting performance of aluminum melt. Besides, the stress concentration will arise around inclusions during the metal deformations process, leading to fatigue cracking, and elongation reduction, which can negatively impact the reliability and performance of the final products [1]. To make matters worse, it is almost impossible to avoid the formation of non-metallic inclusions during the preparation of alloys in smelting and refining systems. Sources of inclusions in these processes are the refractory from the melting furnace and the reaction products of the alloying elements. Furthermore, the amount of chemically and physically formed inclusions in the metal depends on the reactivity of the alloying elements and the metal production route [2]. Due to the increasing demands for clear and high-performance aluminum product, it becomes an urgent task to further reduce the level of impurity especially the inclusion in aluminum melts [3, 4].

Today, a number of conventional methods for inclusion removal such as flux refining and filtration are being used to reduce inclusion levels in molten aluminum prior to casting [5]. These methods are principally based on gravity sedimentation/flotation, inclusion adsorption on the surfaces of gas bubbles and filtration. However, due to kinetics as well as operational limitations [6], these methods can hardly meet high efficiency especially for micrometer-sized inclusions removal. Therefore, as the demand for cleaner metals continues to grow, more efficient methods for inclusion removal are needed.

Unlike conventional methods for inclusion removal, super-gravity separation bears advantages of higher efficiency and free-pollution which has attracted more and more attention from researchers. Hiromi Matsubara et al.[7] have separated intermetallic compounds containing iron

in Al-11%Si Alloy by using centrifugal force during solidification, and the result showed that the castings solidified under super-gravity field appeared obvious macroscopic segregation and the reduction ratio of iron reached 87%. Similarly, Lixin Zhao et al.[8] studied the removal of low-content impurities from Al by super-gravity, the microstructures showed that Fe and Si-rich phases enriched and sedimentated at the bottom along the direction of super-gravity field which indicated that super-gravity separation is a higher efficient method to remove impurities. A new approach to separating and enriching perovskite phase from CaO-TiO_2-SiO_2-Al_2O_3-MgO melt by super gravity was investigated by Juncheng Li et al. and Jintao Gao et al.[9, 10]. It was found that TiO_2 can be enriched in the middle and bottom areas of the sample and the recovery ratio of Ti in the concentrate can reach 74.16% by centrifugal enrichment. However, the effect of super-gravity separation on the non-metallic inclusion removal in the molten metal has not yet been researched. Thus, it is necessary to examine the possibility of super-gravity separation of the non-metallic inclusion from metal melt. In this paper, a series of experiments were processed in order to investigate the influence of the gravity coefficient on the inclusion removal in the aluminum melt. Simultaneously, the size distribution of inclusion particles in the solidified sample has also been investigated to discuss the motion of solid particles in the melt under different gravity field.

Experiment

Experimental Apparatus

On the earth, the easiest way to achieve high gravity environment is achieved by the centrifugal force by rotating. Figure 1 displays a schematic diagram of the experimental apparatus used for the separation of solid particles from Al melt in a super-gravity field. This setup consists of a resistance-heated furnace, a counterweight fixed symmetrically onto the horizontal rotor, a rotating system and a temperature control system which can control temperature within the observed precision range of ±3 ℃ with an R type thermocouple.

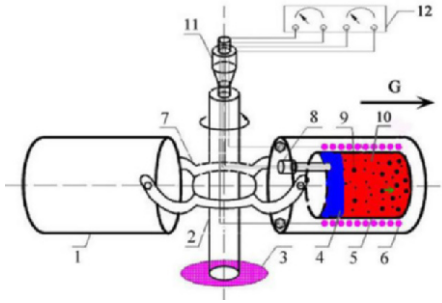

Figure 1. Schematic diagram of the experimental apparatus
1-Counterweight; 2-Centrifugal axis; 3-Base; 4-covering slag; 5-Graphite crucible; 6-Resistance coil; 7-Horizontal rotor; 8-Thermocouple; 9-Solid particles; 10-metal melt; 11-Conductive slipping; 12-Temperature controller

The gravity field size can be characterized by the gravity coefficient which is calculated as the ratio of super-gravitational acceleration to normal-gravitational acceleration via Eq. (1).

$$G = \frac{\sqrt{g^2 + \left(r\omega^2\right)^2}}{g} = \frac{\sqrt{g^2 + \left(\frac{N^2\pi^2 r}{900}\right)^2}}{g} \quad (1)$$

where G is the gravity coefficient ; ω is the angular velocity, $\mathrm{rad \cdot s^{-1}}$; N is the rotating speed of the centrifugal, $\mathrm{r \cdot min^{-1}}$; r is the distance from the centrifugal axis to the center of the sample, in this experiment, $r = 0.25\,\mathrm{m}$; g is the normal gravitational acceleration, $9.8\,\mathrm{m/s^2}$. When $N = 0$ $\mathrm{r \cdot min^{-1}}$, thus $G = 1$

Experimental Method

To figure out the characteristics of the inclusion separation under different gravity field, the experimental procedure was as followed. A356 alloy (15 grams) containing 2.5~3% $MgAl_2O_4$ particles and the covering slag (5 grams) were put into a graphite crucible with the inner diameter of 14 mm as shown in Fig.1 and heated up to a constant temperature of 1023 K, holding 10 min. The covering slag was a mixture of 48% sodium chloride and 52% calcium chloride (mass fraction). Then the centrifugal apparatus was started and adjusted to the specified angular velocity. The centrifugal apparatus was turned off after the sample was treated for 2 min, and then the melt was rapidly cooled by the water spray. Simultaneously, the parallel experiments were carried out at 1023 K for 12 min in the normal gravity field. Samples were cut into two semicircles along the centrifugal force direction, and one was burnished, polished, and made into metallographic specimens for investigating. Optical micrographs were taken along the specific locations on a upright metallurgical microscope (9XB-PC type) and from those, the distributions of area fraction, number density and size of inclusions were measured by using Image-Pro Plus 6.0 professional Image analysis software.

Results and Discussion

Macrostructure of Samples and the Separation Efficiency Obtained by Super Gravity

Figure 2 shows cross-section of the samples obtained by centrifugal treatment with various gravity coefficients. As illustrated in Figure 2(a), under the normal gravity field, uniform structure presents in the sample while there are significant gray regions with inclusion-gathered at the bottom of the samples after centrifugal separated, as shown in Figures 2(b)、(c)、(d)、(e). Moreover, it is found that the particle-accumulated region becomes darker and the thickness of particle-accumulated layer decreases with the increase of gravity coefficient. To clarify the effect of gravity coefficient on the inclusion separation, the separating efficiency can be calculated via Eq. (2).

$$\eta = \left(1 - \frac{S_i}{S_t}\right) \times 100\% \quad (2)$$

where η is the separating efficiency; S_i and S_t are the measured area of the particle-accumulated layer and the total area of the cross-section of the sample. From Table I, it can be seen that the separating efficiency of the sample obviously increases with increase of the gravity coefficient.

When the gravity coefficient G=500, time t=2 min, and temperature T=1023 K, the separating Efficiency of inclusions is up to 90%.

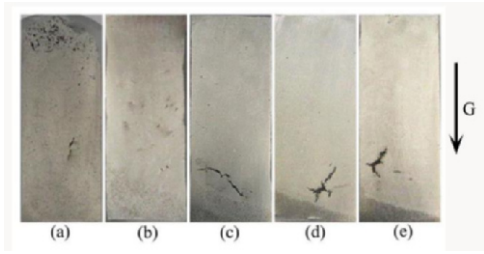

Figure 2. The cross-section of samples obtained by centrifugal treatment with various gravity coefficients: (a) G=1; (b) G=20; (c) G=100; (d) G=308; (e) G=500.

Table I. The thickness of particle-accumulated layer and the separating efficiency of samples in the various gravity fields.

Gravity coefficient G	Thickness of particle-accumulated layer /mm	Separating efficiency η /%
1	32	0
20	7.1	77.8%
100	5.0	84.4%
308	3.5	89.1%
500	3.2	90%

Microstructure of Samples Obtained in the Various Gravity Fields

In order to further study the microstructure of the sample obtained by centrifugal separation, five areas, as shown in Figure 3, were characterized by the metallurgical micrographs, and the corresponding results are given in Figures 4 and 5. It can be seen from the Figure 4 that inclusions almost disperse evenly in the sample without stratification phenomenon. However, all inclusions nearly aggregate to the bottom of the sample which can hardly find any particles in other areas by centrifugal separation at G=500, t=2 min, T=1023 K, as shown in Figure 5. Since the density of inclusion (3.6 g/cm^3) is larger than that of aluminum melt (2.685 g/cm^3) [11], inclusion particles will move to the bottom of the sample with a specific centrifugal force along the super-gravity direction. In addition, the centrifugal force increases with the increase of the gravity coefficient, then the inclusions will migrate easier to the bottom of the sample.

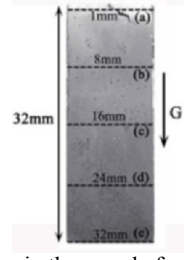

Figure 3. The specific areas in the sample for microstructure observation

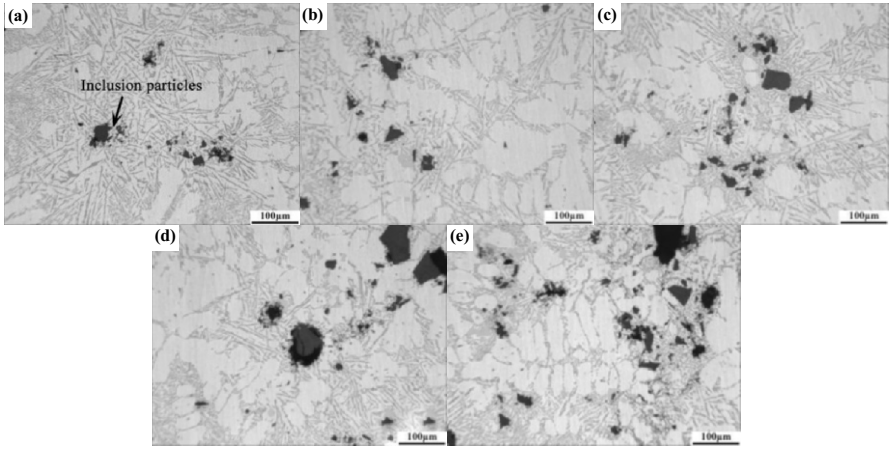

Figure 4. Micrographs of five areas of the sample under the normal gravity field at t=2 min, T=1023 K.

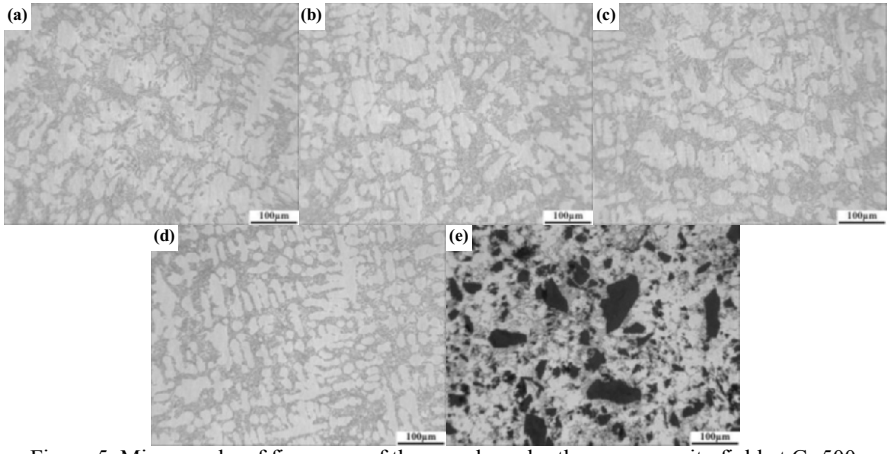

Figure 5. Micrographs of five areas of the sample under the super gravity field at G=500, t=2 min, T=1023 K.

Area Fraction and Number Density of Inclusions in the Sample

In order to further characterize the distribution of inclusions at the different locations in the sample, 20 optical micrographs were taken randomly along the specific locations and from those, the distributions of area fraction and number density of inclusions were measured. Compared with the parallel sample, inclusions distribute in a way of incremental gradient along the direction of super gravity in the sample proceeded by centrifugal force. And the particle distributed gradient in the sample becomes steeper with the increase of the gravity coefficient, as

shown in Figures 6 and 7, because the increased force can drive the inclusion to move faster towards the bottom of the sample in the same time as the gravity coefficient increases.

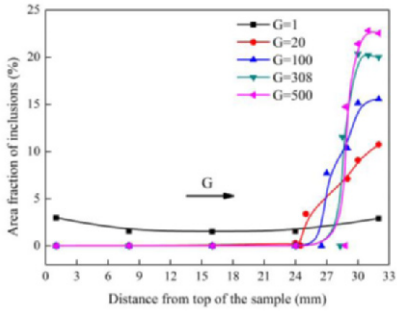

Figure 6. Area fraction of inclusions at different distances from top of the sample.

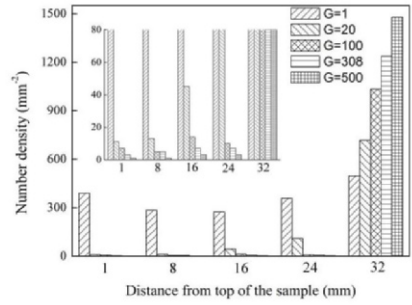

Figure **7.** Number density of inclusions at different locations in the sample.

Inclusion Size Distributions in the Sample after Centrifugal Separation

In the experiments, inclusion size has a wide range in the sample, with the most of inclusions are less than 20 μm and a few larger inclusions can reach 150 μm. Besides, the inclusions were divided into four different sizes, as shown in in Figure 8, and here the aim is to determine the particle size distributions in the sample obtained by centrifugal separation method.

From Figure 8(a), it can be seen that inclusions of differernt sizes still distribute evently in the samples obtained under normal gravity field. While, the number density of inclusions such as size less than 5 μm gradually increases remarkably along the direction of super gravity in the sample proceed under the super gravity field, as shown in Figure 8(b). Moreover, it can hardly find any inclusions with diameter larger than 20 μm in other regions excluding particle-accumulated layer formed at the bottom of the sample obtained by centrifugal separation at G=20, t=2 min, T=1023 K. However, all the inclusions with diameter less than 5 μm will not move to the bottom of the sample until separated with the gravity coefficient G=500, time t=2 min, temperature T=1023 K, as shown in Figure 8(d). It is also known that the motion of solid particles in a viscous liquid under a centrifugal force can be determined by the Stokes' law and the terminal velocity can reach at a very early stage of the centrifugal separation process [12]. The terminal velocity can be expressed as

$$\upsilon_r = \frac{(\rho_P - \rho_L) d^2 G g}{18\eta} \tag{3}$$

where ρ_P, ρ_L, d, and η are density of inclusions, density of matrix melt, inclusion diameter and apparent viscosity, respectively. It is obvious that the velocity of the particle is proportional to the square of the particle diameter and the migration distance is greater in the case of larger particles. Hence, the larger particles are more easily segregated to the bottom of the sample than that of smaller particles.

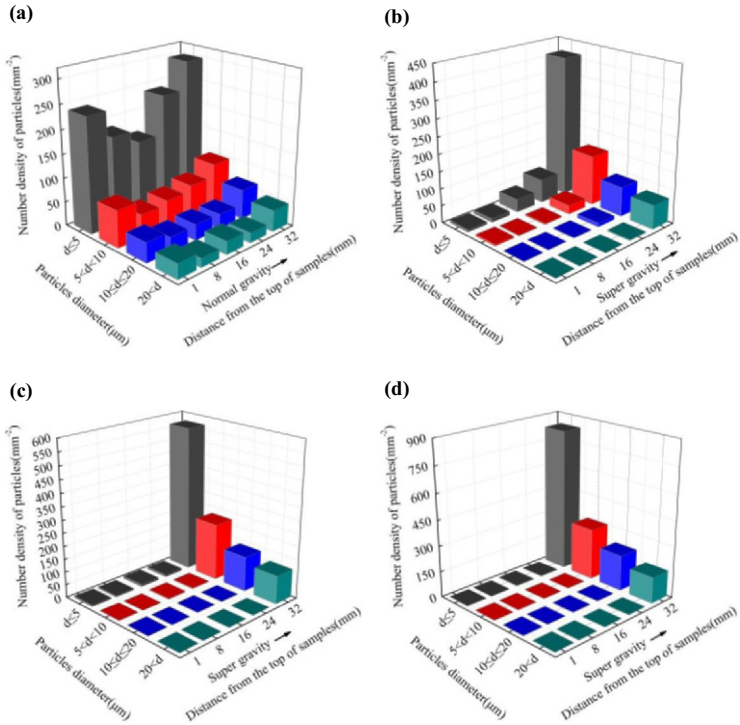

Figure 8. The inclusion distributions in the sample obtained under various gravity field: (a):G=1, (b):G=20, (c):G=100, (d):G=500.

Conclusions

(1) It has been demonstrated that separating non-metallic inclusions from aluminum melt by super gravity is an effective method and inclusions are accumulated at the bottom of samples by super-gravity treatment.
(2) The inclusions are gradually distributed in the sample along the direction of super gravity. Besides, the inclusions distributed gradient in the sample becomes steeper with the increase of the gravity coefficient.
(3) With the gravity coefficient G=500, time t=2 min, and temperature T=1023 K, it is hardly to find any inclusions in the upper and middle areas of the sample and the separating efficiency can reach 90%.
(4) The velocity of the particle is proportional to the square of the particle diameter, therefore, the larger particles can be more easily segregated towards the bottom of the sample.

Acknowledgement

This work was financially supported by the National Natural Science Foundation of China (No. 51234001).

References

1. P.N. Grepeau, “Molten aluminum contamination: gas, inclusions and dress,” *Modern Casting*, 87 (7) (1997), 39-41.

2. N. El-Kaddah, A.D. Patel, and T.T. Natarajan, “The electromagnetic filtration of molten aluminum using an induced-current separator,” *JOM*, 47 (5) (1995), 46-49.

3. S. Shimasaki et al., “Separation of Inclusion Particles from Liquid Metal by Electromagnetic Force,” *13th International Conference on Aluminum Alloys(ICAA13)*, ed. Hasso Weiland, Anthony D. Rollett and William A. Cassada (Pittsburgh, PA: TMS, 2012), 1321-1326.

4. Q.T. Guo et al., “Separation efficiency of alumina particles in Al melt under high frequency magnetic field,” *T NONFERR METAL SOC*, 20 (1) (2010), 153-157.

5. B.W. Zhang, Z.M. Ren, and J.X. Wu, “Continuous electromagnetic separation of inclusion from aluminum melt using alternating current,” *T NONFERR METAL SOC*, 16 (1) (2006), 33-38.

6. F. Frisvold et al., “Removal of Inclusions - A Survey and Comparison of Principles,” *Essential Readings in Light Metals: Cast Shop for Aluminum Production*, 3 (1992), 324-331.

7. Hiromi Matsubara, Norihisa Izawa, and Masura Nakunishi, “Macroscopic Segregation in Al-11 Mass-Si Alloy Containing 2 Mass-Fe Solidified under Centrifugal Force,” *Japanese Journal of Institute of Light Metals*, 48 (2) (1998), 93-97.

8. L.X. Zhao et al., “Removal of Low-Content Impurities from Al By Super-Gravity,” *Metallurgical and Materials Transactions B*, 41 (B) (2010), 505-508.

9. J.C. LI, Z.C. GUO, and J.T. GAO, “Isothermal Enriching Perovskite Phase from CaO–TiO2–SiO2–Al2O3–MgO Melt by Super Gravity,” *ISIJ International*, 54 (4) (2014), 743-749.

10. J.T. GAO, J.C. LI, and Z.C. GUO, “Separation of Perovskite Phase from CaO-TiO2-SiO2-Al2O3-MgO System by Supergravity,” *5th International Symposium on High-Temperature Metallurgical Processing* ed. Tao Jiang and Joseph Lessard (San Diego, CA: TMS, 2014), 67-72.

11. C.G. Kang, and P.K. Rohatgi, “Transient thermal analysis of solidification in a centrifugal casting for composite materials containing particle segregation,” *Metallurgical and Materials Transactions B*, 27 (2) (1996), 277-285.

12. Y. Watanabe, N. Yamanaka, and Y. Fukui, “Control of composition gradient in a metal-ceramic functionally graded material manufactured by the centrifugal method,” *Composites Part A: Applied Science and Manufacturing*, 29 (5) (1998), 595-601.